



Acoustic surveillance of small surface vessels in confined areas

A. Tesei¹, S. Fioravanti², V. Grandi³, P. Guerrini⁴ and A. Maguer⁵

¹ Alessandra Tesei, NATO Undersea Research Centre, Viale San Bartolomeo, 400, 19126, La Spezia (ITALY), tesei@nurc.nato.int

² Stefano Fioravanti, NATO Undersea Research Centre, Viale San Bartolomeo, 400, 19126, La Spezia (ITALY), steve@nurc.nato.int

³ Vittorio Grandi, NATO Undersea Research Centre, Viale San Bartolomeo, 400, 19126, La Spezia (ITALY), grandi@nurc.nato.int

⁴ Piero Guerrini, NATO Undersea Research Centre, Viale San Bartolomeo, 400, 19126, La Spezia (ITALY), guerrini@nurc.nato.int

⁵ Alain Maguer, NATO Undersea Research Centre, Viale San Bartolomeo, 400, 19126, La Spezia (ITALY), maguer@nurc.nato.int

Abstract— Detection of surface vessels is important in confined areas where maritime traffic needs to be carefully monitored. Nowadays, the presence of large ships can be easily detected and accurately monitored either by radar or via AIS system. However, small vessels may be easily missed by usual monitoring systems. The paper describes an acoustic system designed for their detection and localization. It is based on two bottom moored volumetric acoustic arrays and provides both bearing and range estimates of the vessels, as well as their motion tracks. At-sea results demonstrate the system capability for detecting/localizing small vessels in a shallow-water harbor environment.

Index Terms— Acoustics, Harbour, Surface vessels, Surveillance

1. Introduction

The detection, localization and tracking of surface vessels for surveillance and monitoring purposes is of great interest in areas such as marine natural parks and harbors, where navigation is limited and should be controlled. Currently, the presence of large ships in an area of interest can be easily detected and accurately monitored either by radar or via AIS (Automatic Identification System) system.

However, small vessels do not adopt the AIS system and some of them, in particular inflatable boats, have very weak radar signature, hence may be missed by usual monitoring systems. In these cases an alternative useful surveillance method can be based on the detection of underwater acoustic noise radiated by vessels.

The acoustic signatures of small- to mid-sized surface vessels (ranging from inflatable

boats to fishing boat and tugs) are much less reported in the literature than those of large ships, and can be extremely diverse. The knowledge of those signatures is required for the design of the acoustic system for detection and localization.

This paper presents a general characterization of the noise radiated from small boats as the sum of broadband noise and tonal frequencies. Examples of at-sea radiated noise from small vessels are given and demonstrate the validity of the model.

The next part of the paper is dedicated to the description of the system designed and built at the NATO Undersea Research Centre (NURC) for the detection, localization and tracking of small surface vessels. It is based on two identical bottom-moored platforms connected to shore via two electro-optical cables. Each platform hosts a sparse volumetric array of four broadband hydrophones.

A description of the detection algorithms optimized for small- and mid-sized boats is thereafter given. Techniques using either single hydrophone data or the array of hydrophones data are described. Eventually, results are shown from at-sea data which demonstrate the capability of the acoustic system to detect and accurately estimate the direction of arrival of small vessel crafts in a shallow-water harbor environment.

2. Small vessel craft acoustic characterization

Very limited work has been done to characterize the radiated noise from small vessels. The acoustic signatures of small- to mid-sized surface vessels (ranging from inflatable boats to fishing boats and tugs) can be extremely diverse; a general characterization may be the following: with respect to slow, large ships, they commonly have lower levels that may range between 100 and 170 dB/1 μ Pa

@1m, and are characterized by a broader frequency content (up to several tens of kHz) and much higher fundamental frequencies (from hundreds of Hz up to 5-6 kHz), as reported in Table 1. Table 1 lists a set of vessel types and measured characteristics (i.e., fundamental frequency and source level), as found in literature [1]. The model of vessel-radiated noise represented as a sum of broadband noise and low-frequency tones will be assumed to describe the noise radiated from small boats.

Table 1. Selection of classes of surface vessels with related radiated fundamental frequencies and SL values

Vessel type	Frequency (kHz) and SL (dB re 1 μ Pa @1m)
Rigid inflatable (rescue craft)	6.3; 152
7m outboard motor boat	0.63; 156
Fishing boat	0.25-1; 151
Fishing trawler	0.1; 158
Tug pulling loaded barge	1-5; 170-161
Super tanker (266m)	0.008; 187
Container (275m)	0.008, 181

Table 2. Model of fundamental frequencies from engine and propeller of a vessel

Engine Rates	Propeller Rates
Cylinder Firing Rate $f_{CF} = f_{CR}/2$ for 4-stroke engines $f_{CF} = f_{CR}$ for 2-stroke engines	Shaft Rotation Rate $f_{SR} = f_{CR}/A_g$ $A_g = \text{Gear Ratio}$
Crankshaft Rotation Rate $f_{CR} = RPM/60$ $RPM = \text{Engine Speed}$	Blade Rotation Rate $f_{BR} = N_b f_{SR}$ $N_b = \text{Number of Blades}$
Engine Firing Rate $f_{EF} = N_c f_{CF}$ $N_c = \text{Number of Cylinders}$	

The sinusoidal tonal signals can be related to details about the ships engine and propeller (shaft and blade rates), and are the fundamental components of a harmonic set. Table 2 shows the major contributions to the tones from the ship's engine and propeller. The broadband

noise is mainly generated by propeller cavitation, but also by impulsive events in the engine, such as the impact of a piston against the cylinder wall.

Figure 1 shows the Power Spectral Density (PSD) measured from an inflatable boat running at about 18 kn, compared to the PSD of ambient noise in the area of measurements. Although narrow spectral lines are still present at low frequency (below 8 kHz in this case) the level remains high over a wide band and only slowly decays, as confirmed by the spectrogram in Fig. 2. This behavior significantly deviates from the conventional model of big ship SPDs according to which the level decays of 6 dB/oct. beyond 1 kHz.

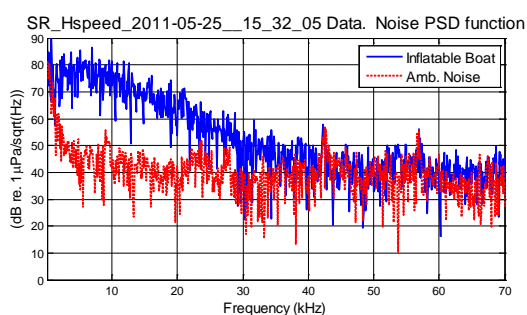


Figure 1. PSD function measured for a rubber boat at 18 knots speed, compared to the PSD of ambient noise

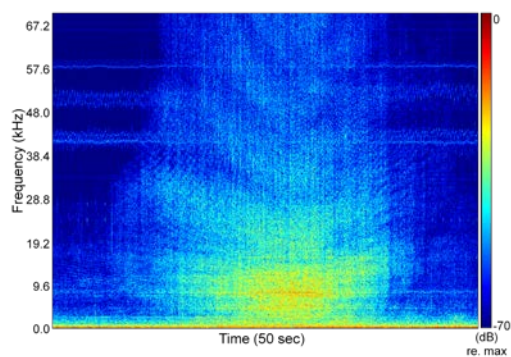


Figure 2. Spectrogram of an inflatable boat in the frequency band 0-70 kHz.

The spread of noise characteristics from vessel to vessel generally implies the need for detection methods different from the conventional methods of ship acoustic detection, and customizing them for the particular problem. Furthermore the spread of possible characteristics of mid- and small-sized vessels makes the problem of classification quite complicated.

3. Acoustic system design

The proposed system for underwater passive acoustic monitoring consists of two identical bottom moored platforms connected to shore via two electro-optical cables which provide DC power to the underwater units and high speed optical links to the shore equipment. Each platform hosts a four hydrophones broadband array. The platform attitude is monitored by an integrated depth, compass, pan and tilt sensor package. Figure 3 shows an illustration of a typical geometry set up of the system for surface vessel monitoring.

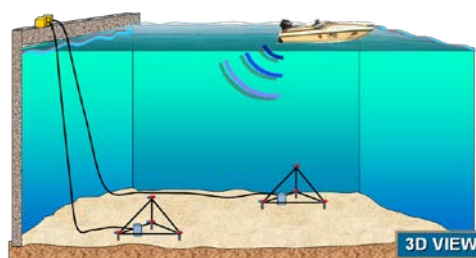


Figure 3. Geometry set-up for experimentation

In-line preamplifiers provide the transducer signals with adequate gain. The signals from the hydrophone preamplifiers are to feed an instrumented pressure vessel containing the acquisition electronics. After further amplification and filtering, the signals are simultaneously digitized by four ultra low-

noise sigma-delta 24 bits A/D converters at a sampling frequency of 192 KHz. An FPGA (Field-programmable Gate Array) based data streamer board provides real-time data serialization and formatting and feeds a fiber optic transmitter which in turn drives the 50/125 μ m fiber optic cable.

Both acoustic and non-acoustic data are received by the shore electronics which provides housekeeping monitoring and control along with an USB 2.0 connection to a host PC for further data storage and processing.

Two of the preamplified hydrophones of the digital volumetric array are shown in Figure 4. The hydrophones are *J&S* spherical transducers model JS-B100-E4DS, measuring 20 mm in diameter, and featuring a fairly flat frequency response within ± 5 dB up to 70 KHz, with resonance frequency at 100 kHz, as shown in Figure 5. An in-line preamplifier provides the transducer signal with a fixed gain and an electronic noise level on the order of $3.0\text{nV}/\sqrt{\text{Hz}}$ @ 40 KHz with a flat response in the bandwidth 20 Hz to 80 KHz.



Figure 4. Two of the preamplified analog hydrophones of a tetrahedron

The non-acoustic sensors (NAS) consist of a *Measurement Specialties* model MSP 340 temperature compensated depth sensor ranging up to 700 Bar and an *OceanServer* model OS5000 3-Axis Solid State digital compass with integrated full rotation Roll & Pitch sensor. The NAS data are sent through an

RS232 link to the acquisition electronics and embedded into the acoustic data stream.

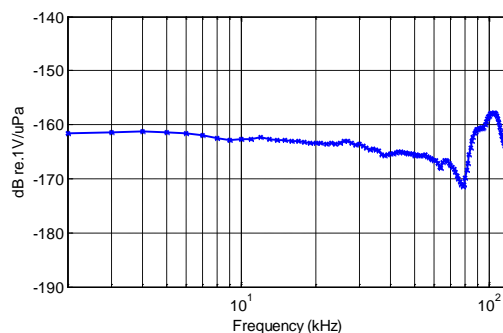


Figure 5. Frequency response of one of the preamplified hydrophones

Each hydrophone of a tetrahedron array (Fig. 6) is connected to a 2-channel A/D converter with two possible gain settings, one Low gain suitable for acquiring high-pressure-level signals and one High gain, suitable for weak signals. The high-gain configuration is characterized by very-low-level input noise. A user-friendly man-machine interface allows the user to select the acquisition of the wished number of channels up to a maximum of 8 (2 gains for each of the four hydrophones) at the same time, and to monitor in real time the data acquired by any of the channels in time, frequency and time-frequency domains.

The Receiving Unit, in addition to providing the electrical DC power to the underwater unit, is responsible for:

- Opto-electrical conversion of the incoming data stream;
- Deserialize the data into a parallel format suitable for data storage and processing;
- High speed USB 2.0 data link to an host computer;
- Extracting the NAS information from the data stream and making them available in RS232 format;
- Allowing GPS time information to be merged with the acoustic data for subsequent timing purpose;

- 16 bits D/A conversion of the four acoustic channels for data monitoring and troubleshooting.



Figure 6. Four-hydrophone volumetric array (tetrahedron) with electronics

4. Methodology of vessel detection and estimation of direction of arrival

As the problem is to detect any kind of unknown surface vessel in the area of measurement, no assumption about the signal shape or autocorrelation function can be made; hence, the approaches are limited to so-called *anomaly detectors* based on the computation of different variables, such as energy, or integrals of higher-order cumulants [2,3] in the case of data from a single hydrophone, and cross-correlation between pairs of hydrophones [4,5] in the case of a sparse volumetric array such as a tetrahedron. Using a single hydrophone allows one to detect the event of the presence of one or more noise sources; using more hydrophones in a 3D sparse array allows one to simultaneously detect the presence of more noise sources, and distinguish among them by estimating their directions of arrival.

The block diagram describing the detection scheme developed for single hydrophone data is shown in Fig. 7, which is based on the evaluation of three different test variables obtained from the computation of second and third order cumulants. The decision test selected is a Generalized Likelihood Ratio Test (GLRT). Details on the computation of the decision test variables λ_{SP}^2 (conventional energy test), $\lambda_{BSP,s}^2$ and λ_{BSP}^2 (both based on bispectrum computation) are given in [6]. A detection is declared if any of the variables overcomes the respective pre-defined threshold, computed on the basis of a given probability of false alarm P_{FA} .

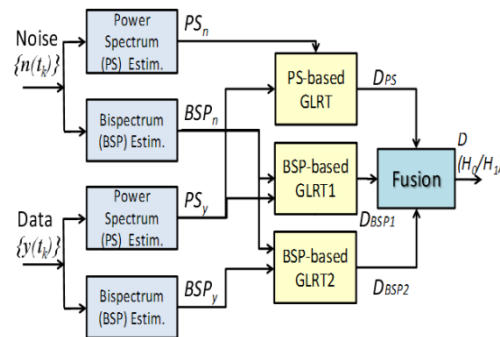


Figure 7. Block diagram of proposed detection method using single hydrophone data.

The signal processing approach developed on the basis of data from the four hydrophone of an underwater measurement station aims at simultaneously detecting and estimating the direction of arrival of an unknown number of noise sources (small surface vessels). The algorithm exploits signal coherence between pairs of hydrophones of the array through cross-correlation [5]; the approach of direction of arrival estimation is based on the time difference of arrival of radiated noise at the hydrophones (T-DOA method). For each pair

of hydrophone processed, if ΔT is the time delay estimated from data cross-correlation, the bearing angle θ is computed as [5] $\theta = \cos^{-1}(\Delta T c_w / d)$, where c_w is the water sound speed at the hydrophones and d the pair distance. This approach requires high sampling frequency and sparse hydrophones ($d \gg \lambda$, if λ is the noise maximum wavelength).

The algorithm block diagram is shown in Fig. 8. Preprocessing of all hydrophone data includes band-pass filtering between 2 kHz and 40 kHz, which is the most significant bandwidth of noise radiation of small boats according to Fig. 1 in the sea environment of the conducted experiment. Cut-off frequencies may vary depending on a preliminary analysis of the local environment. The method is iterative and starts with a separate estimation of azimuth and elevation of the position of each vessel during time.

At the beginning, the comparison between the cross-correlograms images *bearing vs. time* obtained from two pairs of hydrophones at the basis of the tetrahedron and the extraction of each noise track gives the number and a non-ambiguous, rough estimation (not compensated by elevation knowledge) of the azimuth of the vessel detected in the area. Extraction of tracks is obtained first by applying a threshold in order to obtain a binary image, by applying few operators of mathematical morphology, including filtering of isolated spots, closing of small holes finally and skeleton extraction, and applying methods of data association in order to resolve between intersecting tracks.

This first, approximated azimuth estimation is used to compensate the first estimation of the elevation of each vessel, derived from the analysis of the two cross-correlograms of pairs of transversal hydrophones (i.e., correlation between the top hydrophone of the tetrahedron with two of the basis hydrophones respectively). The elevation estimates can now feed the second iteration of the azimuth estimation process. The process is repeated iteratively until the current estimate of both azimuth and elevation differ less than a given

threshold from the previous estimates. In shallow waters (10-20 m water depth) the reciprocal compensation between azimuth and elevation is crucial at short distance (less than about 50 m), while it is negligible when the vessel is far away.

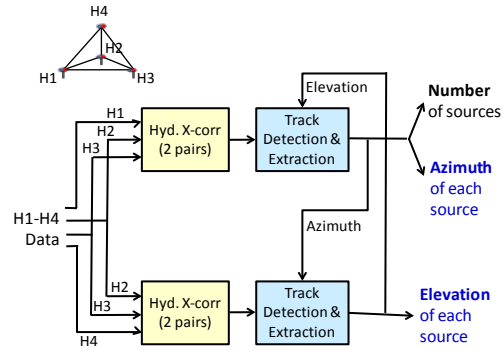


Figure 8. Block diagram of proposed detection and T-DOA methodology.

5. Description of at-sea experiment

Acoustic measurements of ambient noise and passages of surface vessels were conducted in May 2011 in the very shallow, highly anthropic environment of the La Spezia harbor. This environment is characterized by a muddy seabed with smooth, flat bathymetry (water depth between 7 and 12 m). A 1.6m-side tetrahedron of hydrophones was deployed on the seabed, 450m far from the shore lab, in 10.5m of water. The tetrahedron side length implies a maximum theoretical angle resolution of about 0.5° , while the far field is reached at about 85m of range.

For testing the developed detection and direction of arrival algorithms, a controlled set of experiments were conducted. An inflatable boat was equipped with a GPS antenna and a radio link to shore so that the instantaneous position of the vessel could be recorded and integrated into the acoustic data files along each passage of the boat across the

measurement field. An example of track is shown in Fig. 9 when the inflatable boat was running at an approximately constant speed of 18 kn.



Figure 9. Google map of the experimental area, and the GPS track of the passage of an inflatable boat. The tripod location is outlined.

6. Preliminary experimental results and discussion

Preliminary data analysis has been conducted for the validation and refinement of the detection and T-DOA algorithms.

The detection performance from single hydrophone data is considered first. The decision variables λ_{PS}^2 , $\lambda_{BSP,s}^2$ and λ_{BSP}^2 are computed from data of hydrophone 1, during various passages of an inflatable boat in different sub-bands. As an example, the results obtained along the vessel run shown in Fig. 9 are presented in Fig. 10. In each plot a test variable is computed from the acoustic data in a given sub-band along the time of the run, and plotted versus the vessel range (known through its GPS antenna). The test thresholds are superimposed and identified by red dashed lines; P_{FA} is set to 1%. The presence of a vessel is detected every time the test variable

overcomes the corresponding threshold. The maximum detection range obtained for this kind of vessel, at that speed and in that environment is about 500m. Probably due to the particular sound propagation conditions along the run, the maximum detection range is not symmetric when the boat approaches and leaves the tripod. The same behaviour could be found over all runs performed in that direction. The bispectrum seems to provide generally higher signal excess and to allow detection for slightly longer time (and bigger ranges) than the conventional energy test.

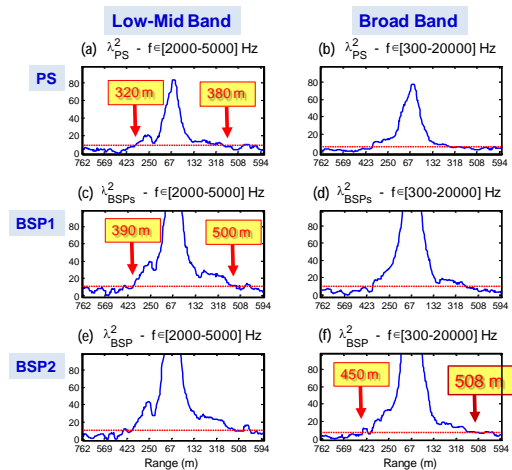


Figure 10. Detection results for a zodiac run. Single hydrophone data.

The preliminary results obtained by the application of the detection and T-DOA algorithm based on the processing of the tetrahedron hydrophones are so far limited to the azimuth estimation without compensation by elevation estimation. Figure 11 shows X-correlogram between hydrophones 1 and 2 at the tripod basis, during part of the same inflatable boat run shown in Fig. 9 (East corresponds to 0° , North to 90°). On the x axis the boat range is given, as measured from the GPS antenna. The left-right ambiguity is still present. Figure 12 shows the track azimuth vs.

range extracted from the data correlation between hydrophones 1 and 3, fused with that one between hydrophones 1 and 2 in order to avoid left-right ambiguity. The true azimuth track measured through the rubber-boat-mounted GPS antenna is superimposed (red, dashed-dotted line). As expected, the lack of elevation compensation is negligible in the far field (i.e., beyond about 90 m of range), while it becomes significant around the closest point of approach (CPA, occurring at about 30m of range in this case).

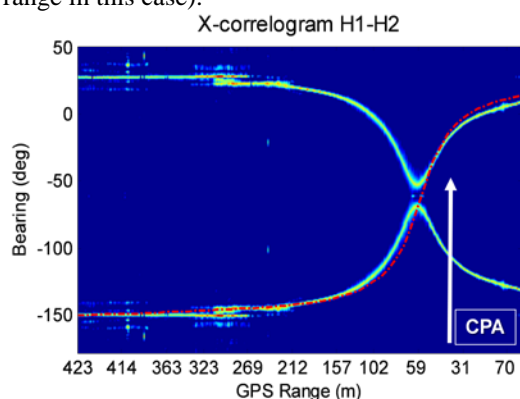


Figure 11. X-correlogram between hydrophones 1 and 2, during the boat run of Fig. 5. Azimuth from GPS in red.

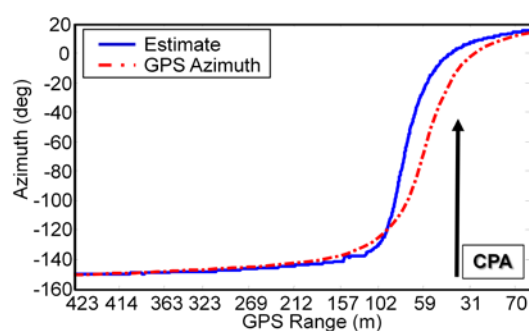


Figure 12. Azimuth estimate from 3 hydrophones compared to GPS measurement.

From the preliminary results shown in Figs. 11 and 12, it seems that the automatic T-DOA approach is more robust than the single hydrophone-based methods, in terms of higher

signal excess at long ranges. An additional significant advantage is the possibility to distinguish among various vessels possibly present in the area at the same time. These considerations will be confirmed through further extensive data analysis.

Acknowledgments

This work is partially funded by EU within the context of the ARGOMARINE Research Project. The authors wish to thank all NURC personnel involved in the design and development of the measurement system and in the conduction of the at sea experiment.

References

- [1] M. Simmonds, S. Dolman, L. Weilgart, eds., 'Oceans of noise' A WDCS Science report, Chapter 3 Sources of marine noise. *Whale and Dolphin Conservation Society (WDCS)*, United Kingdom, 2003.
- [2] M.J., Hinich, G.R., Wilson, 'Detection of non-Gaussian signals in non-Gaussian noise using the bispectrum' *IEEE Tr. on ASSP*, 38 (7), pp. 1126-1131, 1990.
- [3] D., Kletter, H., Messer, 'Suboptimal detection of non-Gaussian signals by third-order spectral analysis' *IEEE Tr. on ASSP*, 38 (6), pp. 901-909, 1990.
- [4] H.F. Silverman, J.M. Sachar, 'The time-delay graph and the delayogram – New visualizations for time delay' *IEEE SP Letters*, 12 (4), pp. 301-304, 2005.
- [5] A. Sutin, B. Bunin, A. Sedunov, N. Sedunov, L. Fillinger, M. Tsionskiy, M. Bruno, 'Stevens passive acoustic system for underwater surveillance' in *Procs. of the 2nd WWS Int. Conf.*, M. di Carrara, Oct. 2010.
- [6] A. Tesei, S. Fioravanti, V. Grandi, P. Guerrini, A. Maguer, 'Acoustic detection of small- and mid-sized surface vessels in very shallow waters' in *Procs. of UAM2011 Int. Conf.*, Kos, June 2011.